JOINT EUROPEAN TORUS

JET–P(90)58

P.H. Rebut, M.Hugon
and JET Team

Magnetic Turbulence Self-Sustainment by Finite Larmor Radius Effect

Magnetic Turbulence Self-Sustainment by Finite Larmor Radius Effect

P.H. Rebut, M.Hugon
and JET Team*

JET-Joint Undertaking, Culham Science Centre, OX14 3DB, Abingdon, UK

* *See Appendix 1*

Preprint of Paper to be submitted for publication in
Plasma Physics and Controlled Fusion

MAGNETIC TURBULENCE SELF-SUSTAINMENT BY FINITE LARMOR RADIUS EFFECT

P. H. Rebut and M. Hugon

JET Joint Undertaking, Abingdon, Oxon, OX14 3EA, United Kingdom

ABSTRACT

A mechanism is proposed for the self-sustainment of a magnetic turbulence resulting from an equilibrium between islands and a chaotic region in a collisionless plasma. It is based on the different behaviour of electrons and ions in the presence of the islands as a result of their different Larmor radii. This effect leads to a difference in their drift velocities and hence to a current which maintains the islands. The mechanism operates for island width smaller than or comparable to the ion Larmor radius. The condition for the self-sustainment of the magnetic turbulence is derived.

I. INTRODUCTION

The particle and energy transport in tokamaks is still not understood. One possible cause for the observed losses is magnetic turbulence (Rechester and Rosenbluth, 1978; Kadomtsev and Pogutse, 1979). In the presence of such a turbulence, the chaotic magnetic field lines provide a radial link between different regions of the plasma. When the turbulence is driven by a mechanism depending on the presence of the turbulence itself, it is self-sustaining above some critical threshold. The self-consistency of this type of turbulence has been recently studied in the case of non-linear microtearing modes. In the collisional regime, these modes are unstable, but they cannot significantly affect the confinement (Garbet et al., 1988). In a collisionless plasma, they can be unstable, when the poloidal β is of the order of unity; they tend to be stabilized by the electric potential associated to the magnetic perturbation, when their non-linear scale is larger than the ion Larmor radius (Garbet et al., 1990).

As shown in an earlier work (Rebut et al.,1987), the magnetic turbulence could result from a mixture of small islands and a chaotic region. This topology may be self-sustained by the difference of resistivity between the chaotic region and the islands, when the electron temperature gradient is larger than a minimum value.

In this paper, another mechanism is proposed for the self-sustainment of this topology in a collisionless plasma. It is based on the different response of electrons and ions to the islands as a result of their different Larmor radii. This differential effect leads to a difference in their drift velocities and hence to a current which sustains the islands.

II. MAGNETIC TOPOLOGY

The calculation is carried out in a slab geometry with the following coordinate system:

$$x = r - r_s \qquad ; \qquad y = r_s \left(\theta - \frac{z}{q_s R}\right) = \frac{\Theta}{k_y} \tag{1}$$

where r, θ and z are the cylindrical coordinates. r_s is the radius of the resonant surface, R is the plasma major radius and $q_s = q(r_s)$ is the safety factor at $r = r_s$. The poloidal wave number k_y is given by $k_y = m/r_s$, where m is the poloidal mode number.

As computed in Rebut and Brusati (1986), islands are embedded in a chaotic zone, when the overlapping parameter γ is between 0.75 and 1.50. For $\gamma \gtrsim 1.50$, the islands are destroyed and the region is fully chaotic. γ is the ratio of the virtual island width 2ε to the distance between two island chains, $\Delta = 1.5q^2/q'm\delta m$, where $q' = dq/dr$ is the shear and δm is the range of poloidal mode numbers around m. Fig.1-a shows a part of a Poincaré map computed by integrating the field line equations with $\gamma = 1.05$. The island is defined by its poloidal extension $2\Theta_0/k_y \le 2\pi/k_y$ and its radial width $2b_0(\Theta_0) \le 2\varepsilon$. It is assumed to be thin, that is $k_y\, b_0(\Theta_0) \ll 1$.

A first integral does not exist in the chaotic zone shown in Fig.1-a. To calculate the effect of the finite ion Larmor radius on the self-sustainment of the turbulence, the region outside the island is modelled by nested surfaces as represented in Fig.1-b. This defines an approximate magnetic flux $\mathcal{A}^*_z$, which is only used to calculate the perturbed electric potential imposed by the presence of the island. The magnetic flux and field describing the island and the chaotic zone are function of Θ_0. In what follows, the dependence on Θ_0 is not shown explicitely. The magnetic flux (or z-component of the vector potential) $\mathcal{A}^*_z$ is defined by:

$$\mathcal{A}^*_z(x,y) = \frac{B'_0}{2} x^2 + \frac{\tilde{\tilde{B}}}{k_y} A(x,y) \tag{2}$$

where $\tilde{\tilde{B}}$ is the amplitude of the perturbing radial field and the shear factor B'_0 is given by:

$$B'_0 = \frac{r_s}{R} B_z \frac{q'(r_s)}{q_s^2} \tag{3}$$

B_z being the toroidal field.

From symmetry, $A(x,y)$ is an even function of y with a period $2\pi/k_y$ and satisfies the normalisation conditions:

$$\begin{cases} A(b_0,0) = 2 \\ A(x,y) = 0 \text{ , when } -\pi/k_y \le y \le -\Theta_0/k_y \text{ and } \Theta_0/k_y \le y \le \pi/k_y \end{cases} \tag{4}$$

The last closed surface of the island is defined by $\mathcal{A}^*_z(x,y) = 0$. From this condition and Eqs.(4), Eq.(2) can be written as:

$$\mathcal{A}^*_z(x,y) = \left(- \frac{\tilde{\tilde{B}}}{k_y}\right) \mathbb{A}(x,y) \quad ; \quad \mathbb{A}(x,y) = 2 \frac{x^2}{b_0^2} - A(x,y) \tag{5}$$

Eq.(5) corresponds to closed surfaces within the island for $-2 \le \mathbb{A} \le 0$ and to periodic surfaces for $\mathbb{A} > 0$ as shown in Fig.1-b. The conditions imposed on $\mathcal{A}^*_z(x,y)$ assume that the following inequality is satisfied:

$$\frac{\tilde{\tilde{B}}}{B'_0} < 0 \tag{6}$$

The function $A(x,y)$ varies slightly with x inside the island and exhibits a slow exponential decay with x outside the island. For $-\Theta_0/k_y \le y \le \Theta_0/k_y$, it can be written:

$$A(x,y) = \begin{cases} \sum_{n=0}^{\infty} a_n \cos(nk_y y) = \mathcal{a}(y) & , \quad \text{for } -b(y) \le x \le b(y) \\ \sum_{n=0}^{\infty} a_n \, e^{-nk_y(|x|-b(y))} \cos(nk_y y) & , \quad \text{for } x \le -b(y) \text{ and } x \ge b(y) \end{cases} \tag{7}$$

where $\pm b(y)$ are the radial coordinates of the island last closed surface given by:

$$b(y) = b_0 \sqrt{\mathcal{a}(y)/2} \tag{8}$$

The x-dependence of $A(x,y)$ outside the island is neglected in Sects. III and IV, but is taken into account in calculating the jump in the derivative of the vector potential across the region associated with the island in Sect. V.

III. PERTURBED ELECTRIC POTENTIAL ASSOCIATED TO A MAGNETIC ISLAND

The ion distribution function depends on the electric potential ϕ. The electron distribution function depends on ϕ and on the magnetic flux $\mathcal{A}_z^*$. In zero Larmor radius MHD, ϕ is a function of $\mathcal{A}_z^*$ and the islands are equipotential. When the finite size of the ion Larmor radius is included, the ions experience an average electric potential ϕ_i different from the potential ϕ_e experienced by the electrons. The electric potential is then no longer a function of $\mathcal{A}_z^*$. The difference between ϕ_e and ϕ_i creates a current along the field lines, and this current sustains the island.

The dependence of the ion density on ϕ_i can be demonstrated as follows. In the reference frame at rest with respect to the islands and in steady state, the continuity equation for the ion guiding centres is :

$$\nabla \cdot (n_i \mathbf{v}_{\parallel i} + n_i \mathbf{v}_{\mathbf{Di}}) = 0 \qquad \text{with:} \qquad \mathbf{v}_{\mathbf{Di}} = \frac{-\nabla\phi_i \times \mathbf{B}}{B^2} \tag{9}$$

where B is the total magnetic field, taken to be constant in magnitude. The ions are assumed not to be in thermodynamic equilibrium along the magnetic field lines because of their mass inertia. Neglecting the average parallel velocity $v_{\parallel i}$ with respect to the drift velocity v_{Di}, Eq. (9) can be written as:

$$\nabla \cdot [n_i (\nabla\phi_i \times \mathbf{B})] = 0 \qquad (10)$$

In the limit of low β, Eq.(10) becomes:

$$(\nabla n_i \times \nabla\phi_i) \cdot \mathbf{B} = 0 \qquad (11)$$

Since n_i and ϕ_i are independent of z, $\nabla n_i \times \nabla\phi_i$ is parallel to $\mathbf{B}$. Therefore, to satisfy Eq.(11), ∇n_i must be parallel to $\nabla\phi_i$ and consequently n_i is a function of ϕ_i, that is:

$$n_i = n_i(\phi_i) \qquad (12)$$

Because their thermal velocity is much larger than the drift velocity $\mathbf{v}_{\mathbf{De}} = (-\nabla\phi_e \times \mathbf{B}) / B^2$, the electrons are in thermodynamic equilibrium in the electric potential ϕ_e along a magnetic field line. As only the part of the electric potential, which is odd with respect to x, contributes to the current sustaining the island (see Section IV), the function of $\mathcal{A}_z^*$, on which depends the electron density, is assumed to be odd with respect to x. Such a function is given by the square root of $\mathbb{A}(x,y)$ defined by Eqs.(5) and (7). $\mathbb{A}(x,y)$ is even with respect to x, being negative inside the island and positive outside. The electron density is then assumed to be independent of $\mathbb{A}$ inside the island, but to depend on the odd function $\pm\sqrt{\mathbb{A}}$ outside, where the upper symbol refers to $x \geq b(y)$ and the lower symbol to $x \leq -b(y)$.

For $\gamma \gtrsim 0.75$, quasi-neutrality is maintained in the chaotic region by equating the electron to the ion flow. This defines the radial electric field $\mathbf{E}_o$ in the reference frame rotating with the islands (Rebut et al.,1986):

$$\mathbf{E}_o = E_0\, \mathbf{e}_x = \frac{KT_e}{q_e} \left(\frac{n'_e}{n_e} + \frac{1}{2} \frac{T'_e}{T_e} \right) \mathbf{e}_x \qquad (13)$$

K is the Boltzmann constant. n'_e and T'_e are the average gradients of electron density n_e and temperature T_e. When taking into account the magnetic island structure explicitly, quasi-neutrality leads to the determination of the perturbed electric potential $\tilde{\varphi}$.

The islands are assumed to be thin and the ion Larmor radius ρ_i is assumed to be of the order of the island half-width b_0, but much smaller than $1/k_y$. Under these conditions, the potential ϕ_i experienced by the ions can be expressed as:

$$\phi_i = - E_0 x + \tilde{\phi}_i(x,y) \quad ; \quad \tilde{\phi}_i(x,y) = b_0\, E_0 \int_{-\infty}^{+\infty} G(x-x')\, \tilde{\varphi}(x',y)\, dx' \qquad (14)$$

$\tilde{\phi}_i$ is the average electric potential felt by the ions having a finite and constant Larmor radius ρ_i at thermal equilibrium in the perturbed potential $\tilde{\varphi}$. The integral containing G(x-x') is the finite ion Larmor radius operator: it is derived in the Appendix by averaging the Fourier components of the perturbed electric field over a gyroperiod and the phase of the motion of a single ion and over a maxwellian distribution of velocities. G(x-x') is defined by Eq. (A.5) and $\tilde{\varphi}(x,y)$ is dimensionless.

As the electron Larmor radius is much smaller than b_0, the electric potential ϕ_e felt by the electrons is given by:

$$\phi_e = - E_0 x + b_0\, E_0\, \tilde{\varphi}(x,y) \qquad (15)$$

The perturbed electric potential $\tilde{\varphi}(x,y)$ is now determined from the requirement of quasi-neutrality inside and outside the island.

III.1. <u>Solution inside the island</u>: $-b(y) \le x \le b(y)$

The electron temperature is assumed to be constant and equal to T_{eo} inside the island. The electron density is a function of ϕ_e only and is given by:

$$n_e = n_e(\phi_e) = n_{eo}\, e^{-(q_e \phi_e / KT_{eo})} \qquad (16)$$

By expanding n_i and n_e as functions of ϕ_i and ϕ_e in the vicinity of 0, the quasi-neutrality condition can be written:

$$q_i n_i(0) + q_e n_e(0) + q_i \frac{dn_i}{d\phi_i}(0)\, \phi_i + q_e \frac{dn_e}{d\phi_e}(0)\, \phi_e + \ldots = 0 \qquad (17)$$

The sum of the first two terms is the quasi-neutrality at the zeroth order and is equal to zero. From Eqs. (12) and (14) and bearing in mind that n_i is mainly a function of x, it can be shown that, whatever ϕ_i, the derivative of n_i with respect to ϕ_i is given by:

$$\frac{dn_i}{d\phi_i}(\phi_i) = - \frac{n_i'}{E_0} \qquad (18)$$

Replacing the derivatives of n with respect to ϕ obtained from Eqs.(16) and (18) into Eq.(17), using the equalities $q_e = -q_i$ and $n_e = n_i$ and dropping the subscript $_0$ in n_{eo} and T_{eo}, we obtain:

$$\frac{n'_e}{n_e}\,\phi_i - \frac{q_e E_0}{KT_e}\,\phi_e = 0 \tag{19}$$

The combination of Eq.(19) with Eqs.(13-15) leads to:

$$\tilde{\varphi}(x,y) = \frac{\frac{1}{2}\frac{T'_e}{T_e}}{\frac{n'_e}{n_e} + \frac{1}{2}\frac{T'_e}{T_e}}\,\frac{x}{b_0} + \frac{\frac{n'_e}{n_e}}{\frac{n'_e}{n_e} + \frac{1}{2}\frac{T'_e}{T_e}}\int_{-\infty}^{+\infty} G(x-x')\,\tilde{\varphi}(x',y)\,dx' \tag{20}$$

III.2. <u>Solution outside the island</u>: $x \le -b(y)$ and $x \ge b(y)$

In this region, the electron density is a function of ϕ_e and $\pm\sqrt{A}$. It is given by:

$$n_e = n_e(\phi_e, \pm\sqrt{A}) = \mathcal{n}_e(\pm\sqrt{A})\; e^{-[q_e\phi_e/KT_e(\pm\sqrt{A})]} \tag{21}$$

with: $\mathcal{n}_e(0) = n_{eo}$ and $T_e(0) = T_{eo}$. The expansion of Eq.(21) at the first order in ϕ_e and $\pm\sqrt{A}$ yields:

$$n_e(\phi_e, \pm\sqrt{A}) = n_{eo} - n_{eo}\frac{q_e\phi_e}{KT_{eo}} + \frac{d\mathcal{n}_e}{d\sqrt{A}}(0)\left(\pm\sqrt{A}\right) \tag{22}$$

By following the procedure used inside the island, the quasi-neutrality condition leads to an expression similiar to Eq.(19), but containing the additional term depending on $\pm\sqrt{A}$, that is:

$$\frac{n'_e}{n_e}\,\phi_i - \frac{q_e E_0}{KT_e}\,\phi_e + \frac{E_0}{n_e}\,\frac{d\mathcal{n}_e}{d\sqrt{A}}(0)\left(\pm\sqrt{A}\right) = 0 \tag{23}$$

Eq.(23) can be transformed with the help of Eqs.(13-15) to an equation for $\tilde{\varphi}(x,y)$. The derivative of $\mathcal{n}_e$ with respect to $\sqrt{A}$ at zero is determined by taking the limit of this equation for small Larmor radii ($G(x-x') = \delta(x-x')$; see Appendix) and for x infinite ($\tilde{\varphi} = 0$ and $\sqrt{A} = \sqrt{2}\,x/b_0$). The expression obtained for $d\mathcal{n}_e(0)/d\sqrt{A}$ is replaced in the equation verified by $\tilde{\varphi}(x,y)$, which becomes:

$$\tilde{\varphi}(x,y) = \frac{\frac{1}{2}\frac{T'_e}{T_e}}{\frac{n'_e}{n_e} + \frac{1}{2}\frac{T'_e}{T_e}} \frac{x}{b_0}\left(1 - \sqrt{1 - \frac{b_0{}^2 a(y)}{2x^2}}\right) + \frac{\frac{n'_e}{n_e}}{\frac{n'_e}{n_e} + \frac{1}{2}\frac{T'_e}{T_e}} \int_{-\infty}^{+\infty} G(x-x')\,\tilde{\varphi}(x',y)\,dx' \tag{24}$$

III.3. Computation of the complete solution

As the main Fourier component of $\tilde{\varphi}(x,y)$ in x has a wave number $k = 1/b_0$, the finite ion Larmor radius operator can be approximated by:

$$\int_{-\infty}^{+\infty} G(x-x')\,\tilde{\varphi}(x',y)\,dx' \simeq \overline{J_0^2}\left[\left(\frac{\rho_i}{b_0}\right)^2\right] \tilde{\varphi}(x,y) = \overline{J_0^2}\,\tilde{\varphi}(x,y) \tag{25}$$

where the function $\overline{J_0^2}$ is defined by Eq. (A.3). This approximation is used in both Eqs. (20) and (24) and $\tilde{\varphi}(x,y)$ can be written as:

$$\tilde{\varphi}(x,y) = \frac{\frac{1}{2}\frac{T'_e}{T_e}}{\frac{n'_e}{n_e}\left(1 - \overline{J_0^2}\right) + \frac{1}{2}\frac{T'_e}{T_e}} \frac{x}{b_0}\left[1 - \mathcal{P}\sqrt{1 - \frac{b_0{}^2 a(y)}{2x^2}}\right] \tag{26}$$

with: $\mathcal{P} = \begin{cases} 0 \text{ for } -b(y) \le x \le b(y) \\ 1 \text{ for } x \le -b(y) \text{ and } x \ge b(y) \end{cases}$

As shown by Eq. (26), the perturbed electric potential $\tilde{\varphi}(x,y)$ is an odd function of x and is independent of y inside the island.

The system of Eqs. (20) and (24) has been solved by numerical iteration. The convergence towards a stable solution for $\tilde{\varphi}(x,y)$ occurs after less than 10 iterations with a relative error smaller than 10^{-2}. The result of such a computation is plotted against x/b_0 in Fig. 2 for the case y = 0, $\rho_i/b_0 = 1$, $n'_e/n_e = 1\ m^{-1}$ and $T'_e/T_e = 2\ m^{-1}$. The vertical slope of $\tilde{\varphi}(x,0)$ just outside the island comes from the fact that the derivative of the term in brackets in Eq. (24) is infinite for $x = \pm b_0$. The analytic expression of $\tilde{\varphi}(x,y)$ given by Eq. (26) agrees with the computed result to within 10%, when $\rho_i/b_0 \gtrsim 1$.

The islands behave as a foreign body in the plasma. Their magnetic surfaces are equipotential for $\overline{J_0^2} = 1$ in the limit of very small Larmor radius from Eqs. (14), (15) and (26) as expected for zero Larmor radius MHD. For $\overline{J_0^2} = 0$ (limit of large ion Larmor radius compared to b_0), inside the island, the electrons only experience the part of the electric field $\mathbf{E_o}$ (Eq. (13)) due to the electron density gradient, whereas the ions experience $\mathbf{E_o}$ as in the chaotic region.

IV. CURRENT DENSITY SUSTAINING THE ISLAND DUE TO FINITE ION LARMOR RADIUS EFFECT

In steady state, the current density conservation requires:

$$\nabla\cdot(J_{\parallel}\mathbf{e_{\parallel}} + n_i q_i \mathbf{v_{Di}} + n_e q_e \mathbf{v_{De}}) = 0 \tag{27}$$

$J_{\parallel}$ is the electron current density along the field lines, being the sum of the constant plasma current density and the perturbed current density, $\delta J_{\parallel}(x,y)$, sustaining the island. $\mathbf{e_{\parallel}}$ is the unit vector parallel to $\mathbf{B}$ and is divergence free. $\mathbf{v_{Di}}$ and $\mathbf{v_{De}}$ are the ion and electron drift velocities respectively.

The x- and y-components of the magnetic field $\mathbf{B}$ are calculated from the curl of $\mathcal{A}^*_z(x,y)\ \mathbf{e_z}$ (Eq. (2)). The leading term of $\nabla\cdot(J_{\parallel}\mathbf{e_{\parallel}})$ is:

$$\nabla\cdot(J_{\parallel}\mathbf{e_{\parallel}}) = -\frac{B_0' x}{B}\ \nabla_y \delta J_{\parallel}(x,y) \tag{28}$$

and consequently other terms in $\nabla\cdot(J_{\parallel}\mathbf{e_{\parallel}})$ are neglected. In the case of thin islands ($k_y b_0 \ll 1$), $B_0' x$ is larger than the derivatives of $\tilde{\tilde{B}}\ A(x,y) / k_y$ with respect to x and y in absolute value.

From the definition of $\mathbf{v_{Di}}$ (Eq. (9)) and in the limit of low β, $\nabla\cdot(n_i q_i \mathbf{v_{Di}})$ is zero, since n_i is a function of ϕ_i. Under the same conditions and taking account of quasi-neutrality $n_e = n_i$, it follows that:

$$\nabla\cdot(n_e q_e \mathbf{v_{De}}) = -\frac{q_e}{B^2}\ \mathbf{B}\cdot\left(\nabla n_i \mathbf{x} \nabla\phi_e\right) \tag{29}$$

The main component of the magnetic field $\mathbf{B}$ is in the z-direction. ∇n_i is equal to $dn_i/d\phi_i\ \nabla\phi_i$, where $dn_i/d\phi_i$ is defined by Eq. (18). Using the definitions of the potentials given by Eqs. (14-15), it can be shown that the leading term of $\mathbf{\nabla}\cdot(n_e q_e \mathbf{v_{De}})$ depends on $\nabla_y \tilde{\varphi}(x,y)$.

After combination with Eq. (28) and the expressions for $\mathbf{\nabla}\cdot(n_i q_i \mathbf{v_{Di}})$ and $\mathbf{\nabla}\cdot(n_e q_e \mathbf{v_{De}})$, Eq. (27) becomes:

$$\nabla_y \delta J_{\parallel}(x,y) = -\frac{q_e E_0}{B_0'} n_e' \frac{b_0}{x} \nabla_y \left(\tilde{\varphi}(x,y) - \int_{-\infty}^{+\infty} G(x-x')\, \tilde{\varphi}(x',y)\, dx' \right) \tag{30}$$

The solution for $\delta J_{\parallel}(x,y)$ is equal to the integral of the right-hand side of Eq. (30) with respect to y plus a function of $\mathcal{A}_z^*$. This function is taken to be $C_1(\mathcal{A}_z^*)$ inside the island and $C_2(\mathcal{A}_z^*)$ different from $C_1(\mathcal{A}_z^*)$ outside. Both functions are defined by other phenomena such as collisions for example: the resistivity is assumed to the same inside and outside the island. Then, $C_1(\mathcal{A}_z^*)$ and $C_2(\mathcal{A}_z^*)$ are determined from the condition that the perturbed current is zero on each magnetic surface inside the island and is zero on average in the chaotic region taking account of all island chains. Because of the diffusion of the chaotic field lines, $C_2(\mathcal{A}_z^*)$ is chosen to be a constant C_2. C_2 has a sign opposite to the integral of the right-hand side of Eq. (30).

The self-sustainment condition is independent of the addition of any constant current density everywhere in the plasma (see Section V). $\delta J_{\parallel}(x,y)$ is taken to be equal to the above solution minus the constant C_2. Using the data of $\tilde{\varphi}(x,0)$ shown in Fig. 2, $\delta J_{\parallel}$ has been computed and normalised values are plotted as a function of x/b_0 in Fig. 3. It is an even function of x.

By neglecting the variations of $\delta J_{\parallel}(x,y)$ as a function of x and y inside the island and by using the approximation for the finite ion Larmor radius operator (Eq. (25)) and the definition of $\tilde{\varphi}(x,y)$ (Eq. (26)), $\delta J_{\parallel}(x,y)$ can be written as:

$$\delta J_{\parallel}(x,y) = -\frac{q_e E_o}{B'_o} n'_e \frac{1}{2}\frac{T'_e}{T_e} \frac{\left(1 - \overline{J_o^2}\right)}{\frac{n'_e}{n_e}\left(1 - \overline{J_o^2}\right) + \frac{1}{2}\frac{T'_e}{T_e}} .$$

$$\begin{cases} \left(1 - \sqrt{1 - \dfrac{b_o{}^2 a(y)}{2x^2}}\right) & \text{for } x \le -b(y) \text{ and } x \ge b(y) \\ \dfrac{\pi C(\Theta_o) - \pi + 2}{2} & \text{for } -b(y) \le x \le b(y) \end{cases} \qquad (31)$$

with:

$$C(\Theta_o) = \frac{(\pi-2)\Delta}{\pi\Delta - 2b_o \int_0^{\Theta_o} \sqrt{\dfrac{a(y)}{2}}\, d(k_y y)} \qquad (32)$$

The perturbed current density sustaining the island, $\delta J_{\parallel}(x,y)$, results from the difference between the electric potentials experienced by the electrons and the ions.

V. MAGNETIC CHAOS SELF-SUSTAINMENT

Ampère's law for thin islands ($k_y\ b_o \ll 1$) can be written as:

$$\frac{\tilde{\tilde{B}}}{k_y} \nabla_x^2 A(x,y) = -\mu_o\ \delta J_{\parallel}(x,y) \qquad (33)$$

Integration of Eq.(33) over x across the region associated with the island yields:

$$\frac{\tilde{\tilde{B}}}{k_y}\left(\nabla_x A(x_o,y) - \nabla_x A(-x_o,y)\right) = -\mu_o \int_{-x_o}^{+x_o} \delta J_{\parallel}(x,y)\, dx \qquad (34)$$

The boundary x_o is infinite here, since $\delta J_{\parallel}(x,y)$ is zero at infinity. In the case where $\rho_i/b_o \gtrsim 1$, the perturbed current is defined by Eqs.(31-32) and its integral is calculated to be:

$$\int_{-\infty}^{+\infty} \delta J_{\parallel}(x,y)\, dx = - \frac{n_e q_e E_0}{B_0'} \frac{1}{2} \frac{T_e'}{T_e} \frac{n_e'}{n_e} \frac{\left(1 - \overline{J_0^2}\right)}{\frac{n_e'}{n_e}\left(1 - \overline{J_0^2}\right) + \frac{1}{2}\frac{T_e'}{T_e}} \pi\, C(\Theta_0)\, b(y) \qquad (35)$$

By taking into account the x-dependence of $A(x,y)$ outside the island only in the calculation of its derivative (see Eq. (7)), the matching between the internal and external solutions for $A(x,y)$ is expressed as:

$$\nabla_x A(x_0,y) - \nabla_x A(-x_0,y) = \sum_{n=0}^{\infty} (-2nk_y)\, a_n \cos(nk_y y) \qquad (36)$$

Combination of Eqs. (34-36) leads to:

$$\sum_{n=0}^{\infty} n\, a_n \cos(nk_y y) = - \frac{\mu_0}{\approx\!\!B} \frac{n_e q_e E_0}{B_0'} \frac{1}{2} \frac{T_e'}{T_e} \frac{n_e'}{n_e} \frac{\left(1 - \overline{J_0^2}\right) \pi\, C(\Theta_0)}{\frac{n_e'}{n_e}\left(1 - \overline{J_0^2}\right) + \frac{1}{2}\frac{T_e'}{T_e}} \frac{b(y)}{2} \qquad (37)$$

for $-\Theta_0/k_y \le y \le \Theta_0/k_y$.

Eq. (37) is solved by computing the Fourier components a_n and using the normalisation condition obtained from Eqs. (4) and (7) (Rebut and Hugon, 1985):

$$\sum_{n=1}^{\infty} a_n \left(1 - \cos(n\Theta_0)\right) = 2 \qquad (38)$$

Eq. (37) is then equivalent to:

$$- \mu_0 \frac{n_e q_e E_0}{B_0'} \frac{1}{2} \frac{T_e'}{T_e} \frac{n_e'}{n_e} \frac{\left(1 - \overline{J_0^2}\right)}{\frac{n_e'}{n_e}\left(1 - \overline{J_0^2}\right) + \frac{1}{2}\frac{T_e'}{T_e}} = \frac{\approx\!\!B}{b_0\, C(\Theta_0)\, D(\Theta_0)} \qquad (39)$$

with:

$$D(\Theta_0) = \frac{1}{2} \sum_{n=1}^{\infty} \left(\frac{1 - \cos(n\Theta_0)}{n}\right) \int_0^{\Theta_0} \sqrt{\frac{a(y)}{2}} \cos(nk_y y)\, d(k_y y) \qquad (40)$$

$C(\Theta_0)$ defined by Eq. (32) and $D(\Theta_0)$ are computed by iterations starting from a trial function. Usually, the calculation requires less than 10 iterations to converge for an accuracy of 10^{-3}. The plot of $D(\Theta_0)$ against Θ_0 is presented in Fig. 4.

$\tilde{\tilde{B}}$ and b_0 are determined from Poincaré map computations (see Fig. 1-a). The relationships between these parameters and those relevant to the Poincaré map calculation, $\tilde{\tilde{B}}_{MAP}(\Theta_0)$ and $b_{MAP}(\Theta_0)$, are:

$$\tilde{\tilde{B}}_{MAP}(\Theta_0) = \frac{\tilde{\tilde{B}}}{B'_0 k_y \Delta^2} \quad ; \quad b_{MAP}(\Theta_0) = \frac{b_0}{\Delta} \tag{41}$$

$\tilde{\tilde{B}}_{MAP}(\Theta_0)$ is always negative because of inequality (6).

With Eqs. (13) and (41), Eq. (39) is transformed into:

$$\mu_0 \frac{n_e K T_e}{B_0'^2} \frac{1}{2} \frac{T'_e}{T_e} \frac{n'_e}{n_e} \frac{\left(\frac{n'_e}{n_e} + \frac{1}{2}\frac{T'_e}{T_e}\right)\left(1 - \overline{J_0^2}\right)}{\frac{n'_e}{n_e}\left(1 - \overline{J_0^2}\right) + \frac{1}{2}\frac{T'_e}{T_e}} \frac{1}{k_y \Delta} = F(\Theta_0) \tag{42}$$

with:

$$F(\Theta_0) = \frac{-\tilde{\tilde{B}}_{MAP}(\Theta_0)}{C(\Theta_0)\, D(\Theta_0)\, b_{MAP}(\Theta_0)} \tag{43}$$

In the limit of very large Larmor radii, $\overline{J_0^2}$ is zero and the left-hand side of Eq. (42) is maximum. This equation becomes:

$$\mu_0 \frac{n_e K T_e}{B_0'^2} \frac{1}{2} \frac{T'_e}{T_e} \frac{n'_e}{n_e} \frac{1}{k_y \Delta} = F(\Theta_0) \tag{44}$$

The left-hand side of Eq. (42) is proportional to the poloidal β and is independent of the sign of the shear q'. It is zero when: 1)-the electron temperature gradient T'_e and consequently the perturbed electric potential $\tilde{\varphi}(x,y)$ are zero; 2)-the electron density gradient n'_e is zero; 3)-the radial electric field E_0 is zero (this occurs for islands separated by nested magnetic surfaces ($\gamma \lesssim 0.75$) or for $n'_e/n_e = -(1/2)\, T'_e/T_e$); or 4)-$\overline{J_0^2}$ is equal to 1 as is the case for ion Larmor radii much smaller than the island size.

The procedure to determine $F(\Theta_0)$ is the following. A Poincaré map is first calculated for a given value of the overlapping parameter γ. The poloidal extension $2\Theta_0$ of the island is measured on the map. The corresponding function $\alpha(y)$ (Eq.(7)) is obtained by computing the Fourier components a_n with the iterative code. This function together with Eq.(2) define the magnetic field, which is used to compute other Poincaré maps. $\tilde{\tilde{B}}_{MAP}(\Theta_0)$ is determined by adjusting the amplitude of the perturbed field $\tilde{\tilde{B}}_{MAP}$ to obtain the same value of Θ_0 as on the first map. The island half-width $b_{MAP}(\Theta_0)$ is then measured. The results of computation of these parameters for different values of Θ_0 are reported in Table I with $C(\Theta_0)$, $D(\Theta_0)$ and γ. $\tilde{\tilde{B}}_{MAP}(\Theta_0)$ increases with γ until it reaches a constant amplitude for $\gamma \gtrsim 0.75$. $b_{MAP}(\Theta_0)$ passes through a maximum at $\gamma = 1.0$ before decreasing at large values of γ as a result of the destruction of the island by chaoticity.

Table I shows that $F(\Theta_0)$ increases as Θ_0 decreases, that is as the island is destroyed. Its minimum value compatible with the existence of small magnetic islands embedded in a chaotic region is close to 0.20, corresponding to $\gamma \approx 0.75$, when the last nested surface between the island chains is destroyed. The islands are self-sustained, when the left-hand side of Eq.(42) is larger than 0.20.

VI. CONCLUSION

The magnetic turbulence, which may be responsible for the observed transport in tokamaks, could be an equilibrium between islands and a chaotic zone. A possible mechanism maintaining this turbulence has been proposed in this study. The current sustaining the islands depends on the cross product of the density gradient and the electric field. It is produced by the difference between the electric potentials experienced by the electrons and the ions as a result of their different Larmor radii. The island width is of the order of the ion Larmor radius.

The condition for magnetic turbulence self-sustainment is that the left-hand side of Eq.(42) be larger than 0.20. The left-hand side of Eq.(42) is proportional to the poloidal β and to the gradients of electron temperature and density.

ACKNOWLEDGEMENTS

The authors are very grateful to Dr J.Wesson and Dr D.Baldwin for helpful comments. In addition, fruitful discussions with Drs X.Garbet, F.Mourgues and A.Samain are acknowledged.

REFERENCES

Garbet X., Mourgues F. and Samain A. (1988) Plasma Phys. Contr. Fusion **30**, 343.

Garbet X., Mourgues F. and Samain A. (1990) Plasma Phys. Contr. Fusion **32**, 131.

Kadomtsev B.B. and Pogutse O.P. (1979) Proc. 7th Int. Conf. on Plasma Physics and Controlled Nuclear Fusion Research, Innsbruck, 1978, Vol.I, p.649, IAEA, Vienna.

Rebut P.H. and Brusati M. (1986) Plasma Phys. Contr. Fusion **28**, 113.

Rebut P.H., Brusati M., Hugon M. and Lallia P.P. (1987) Proc. 11th Int. Conf. on Plasma Physics and Controlled Nuclear Fusion Research, Kyoto, 1986, Vol.II, p.187, IAEA, Vienna.

Rebut P.H. and Hugon M. (1985) Proc. 10th Int. Conf. on Plasma Physics and Controlled Nuclear Fusion Research, London, 1984, Vol.II, p.197, IAEA, Vienna.

Rechester A.B. and Rosenbluth M.N. (1978) Phys. Rev. Lett. **40**, 38.

APPENDIX: FINITE LARMOR RADIUS EFFECT ON THE ELECTRIC POTENTIAL EXPERIENCED BY THE IONS

The purpose of this Appendix is to calculate the average potential experienced by ions with a finite and constant Larmor radius at thermal equilibrium in an electric potential perturbation.

Let us consider an ion moving in a constant magnetic field $\mathbf{B} = B\,\mathbf{e_z}$ and an electric field $\tilde{\mathbf{E}} = \tilde{E}(x)\,\mathbf{e_x}$. Generally, the electric field $\tilde{E}$ can be expressed as:

$$\tilde{E}(x') = \frac{1}{\sqrt{2\pi}} \int_{-\infty}^{+\infty} \tilde{E}_k(k)\, e^{ikx'}\, dk \qquad (A.1)$$

k stands for the wave number k_x. By expanding $e^{ikx'}$ in terms of Bessel functions, it can be shown that the k^{th} harmonic of the electric field $\tilde{E}(x')$ averaged over a gyroperiod and the initial phase α of the ion motion is:

$$\langle\langle \tilde{E}_k(k)\, e^{ikx'} \rangle_t \rangle_\alpha = \tilde{E}_k(k)\, e^{ikx}\, J_0^2\!\left(\frac{kv_\perp}{\omega_i}\right) \qquad (A.2)$$

$J_0(z)$ is the zeroth order Bessel function of the first kind. $v_\perp$ is the ion velocity perpendicular to $\mathbf{B}$ and $\omega_i = q_i\, B / m_i$ its gyrofrequency.

For ions at thermal equilibrium at the temperature T, Eq. (A.2) is averaged over a maxwellian distribution of velocities $v_\perp$ leading to the average electric field, $\tilde{E}_L(x)$, felt by the ions in the electric field of Fourier component k, $\tilde{E}(x) = \tilde{E}_k(k)\, e^{ikx}$:

$$\tilde{E}_L(x) = \overline{J_0^2}(k^2\rho_i^2)\, \tilde{E}(x) = e^{-k^2\rho_i^2}\, I_0(k^2\rho_i^2)\, \tilde{E}(x) \qquad (A.3)$$

where $\rho_i = \sqrt{KT/m_i}\, /\, \omega_i$ is the ion Larmor radius and $I_0(z)$ is one of the modified Bessel functions of zeroth order. $\overline{J_0^2}(k^2\rho_i^2)$ is equal to 1 for very small Larmor radii ($\rho_i \ll 1/k$) and tends toward zero for very large ρ_i ($\rho_i \gg 1/k$).

Taking into account all harmonics of $\tilde{E}(x')$, the average electric field $\tilde{E}_L(x)$ can be written as:

$$\tilde{E}_L(x) = \int_{-\infty}^{+\infty} G(x-x')\, \tilde{E}(x')\, dx' \qquad (A.4)$$

This equation defines the finite ion Larmor radius operator, where G(x-x') is equal to:

$$G(x-x') = \frac{1}{(2\pi)^{3/2}} \frac{e^{-\left(\frac{x-x'}{4\rho_i}\right)^2}}{\rho_i} K_0\left(\frac{x-x'}{4\rho_i}\right)^2 \qquad (A.5)$$

The function G(x-x') is normalized to 1. It is plotted against x' for x = 0 and ρ_i = 1 in Fig.5. $K_0(z)$ is the other modified Bessel function of zeroth order behaving as $-\ln(z/2)$, when z approaches 0. Eq.(A.5) shows that the limits of G(x-x') are a delta function $\delta(x-x')$ for ρ_i tending toward zero and zero for ρ_i infinite. The function G(x-x') is even with respect to x-x' and the finite ion Larmor radius operator conserves the parity.

Assuming that $\tilde{E}_L(x)$ and $\tilde{E}(x)$ are derived from the electric potentials $\tilde{\phi}_L(x)$ and $\tilde{\phi}(x)$ respectively, Eq.(A.4) becomes after integration by parts:

$$\nabla_x \tilde{\phi}_L(x) = -\int_{-\infty}^{+\infty} \nabla_{x'} G(x-x')\, \tilde{\phi}(x')\, dx' \qquad (A.6)$$

When the ion temperature is constant, the derivatives of G(x-x') with respect to x and x' are equal and opposite. Integration of Eq.(A.6) over x yields the average electric potential $\tilde{\phi}_L(x)$:

$$\tilde{\phi}_L(x) = \int_{-\infty}^{+\infty} G(x-x')\, \tilde{\phi}(x')\, dx' \qquad (A.7)$$

Table I

Numerical results for the perturbed magnetic field $\tilde{\tilde{B}}_{MAP}(\Theta_0)$ and the island half-width $b_{MAP}(\Theta_0)$ obtained from the Poincaré map computation as a function of Θ_0 and of the overlapping parameter γ. Also shown are the values computed for $C(\Theta_0)$ (Eq. (32)), $D(\Theta_0)$ (Eq. (40)) and $F(\Theta_0)$ (Eq. (43)).

γ	Θ_0	$-\tilde{\tilde{B}}_{MAP}(\Theta_0)$	$b_{MAP}(\Theta_0)$	$C(\Theta_0)$	$D(\Theta_0)$	$F(\Theta_0)$
0.4	0.91π	0.010	0.20	0.50	0.65	0.16
0.7	0.70π	0.030	0.37	0.61	0.67	0.20
1.0	0.44π	0.030	0.40	0.50	0.50	0.30
1.2	0.32π	0.025	0.33	0.44	0.38	0.46
1.4	0.13π	0.030	0.24	0.38	0.16	2.04

Fig. 1: (a) Poincaré map computed for an overlapping parameter γ = 1.05 showing magnetic islands in equilibrium in a chaotic region; the island is defined by its poloidal extension $2\Theta_0/k_y \leq 2\pi/k_y$ and its radial width $2b_0$; Δ is the distance between two island chains. (b) The chaotic zone is modelled by nested magnetic surfaces to define an approximate magnetic flux outside the island.

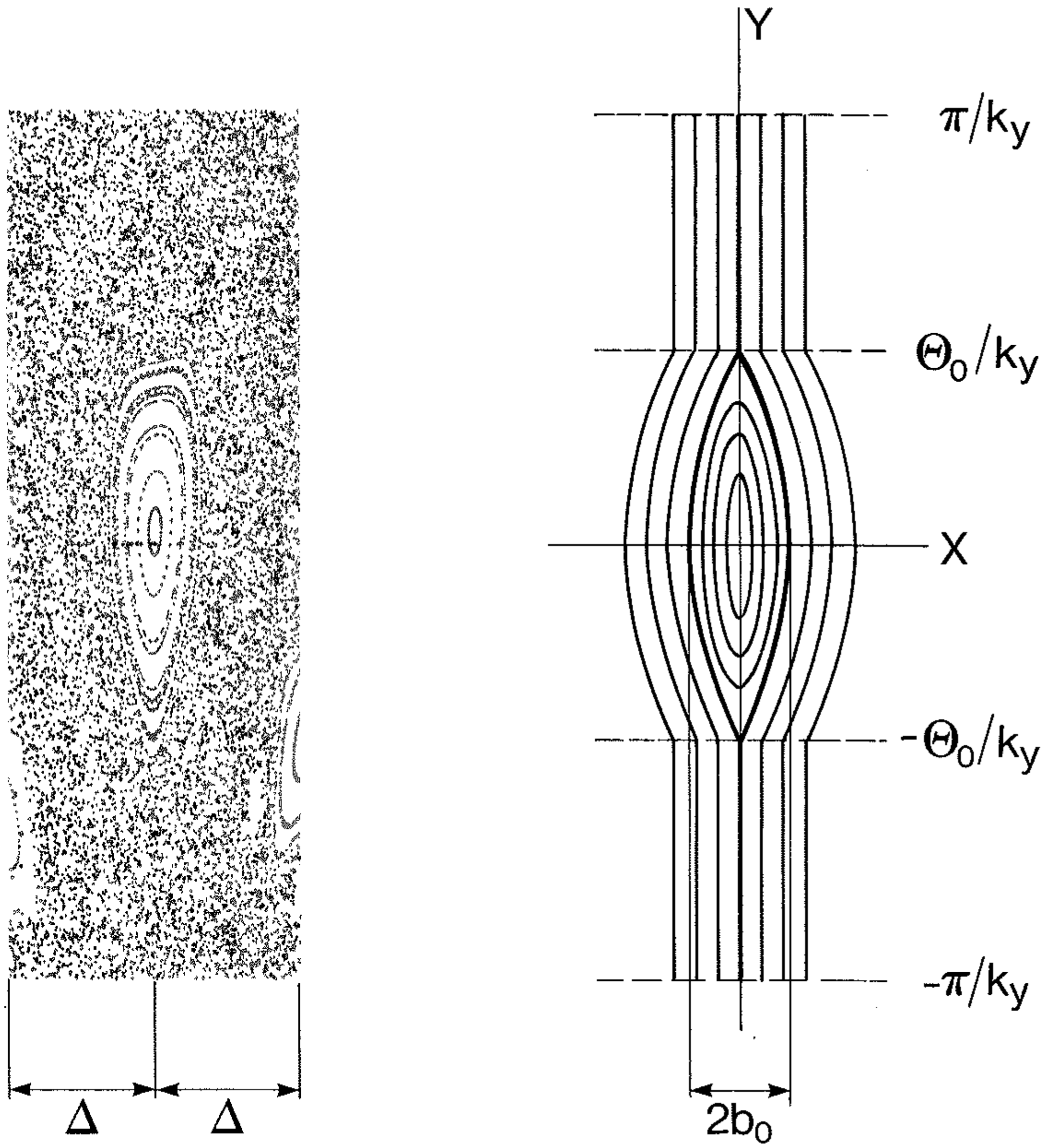

(a) (b)

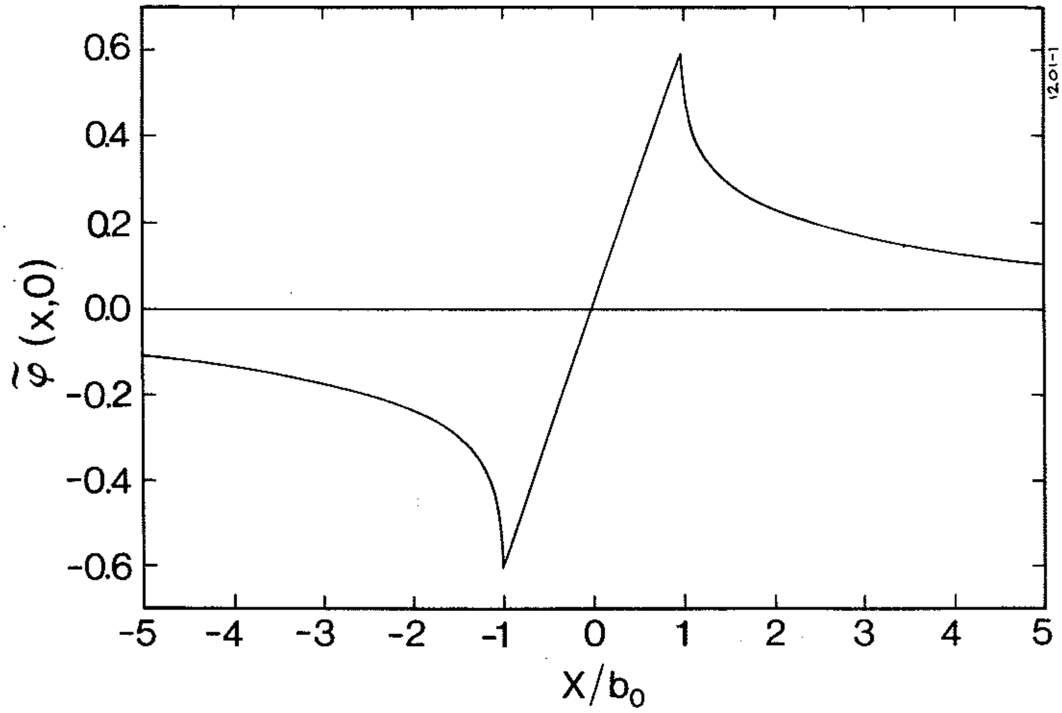

Fig. 2: Computed values for the perturbed electric potential $\tilde{\varphi}(x,0)$. The island lies between $x = -b_o$ and $x = b_o$. The ion Larmor radius ρ_i to island half-width b_o ratio is 1. $n_e'/n_e = 1\ m^{-1}$ and $T_e'/T_e = 2\ m^{-1}$.

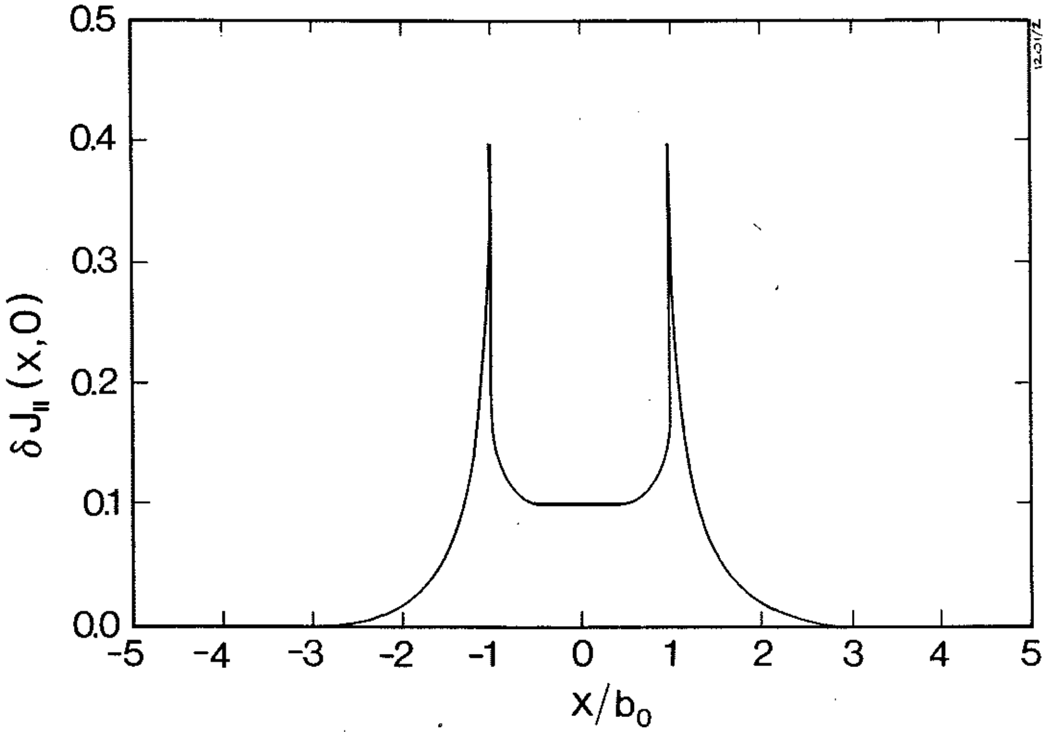

Fig. 3: Current density, $\delta J_{\parallel}(x,0)$, sustaining the island versus x/b_o. $\delta J_{\parallel}(x,0)$ is computed using the data of $\tilde{\varphi}(x,0)$ shown in Fig. 2 and is normalised to $-q_e E_o n_e'/B_o'$.

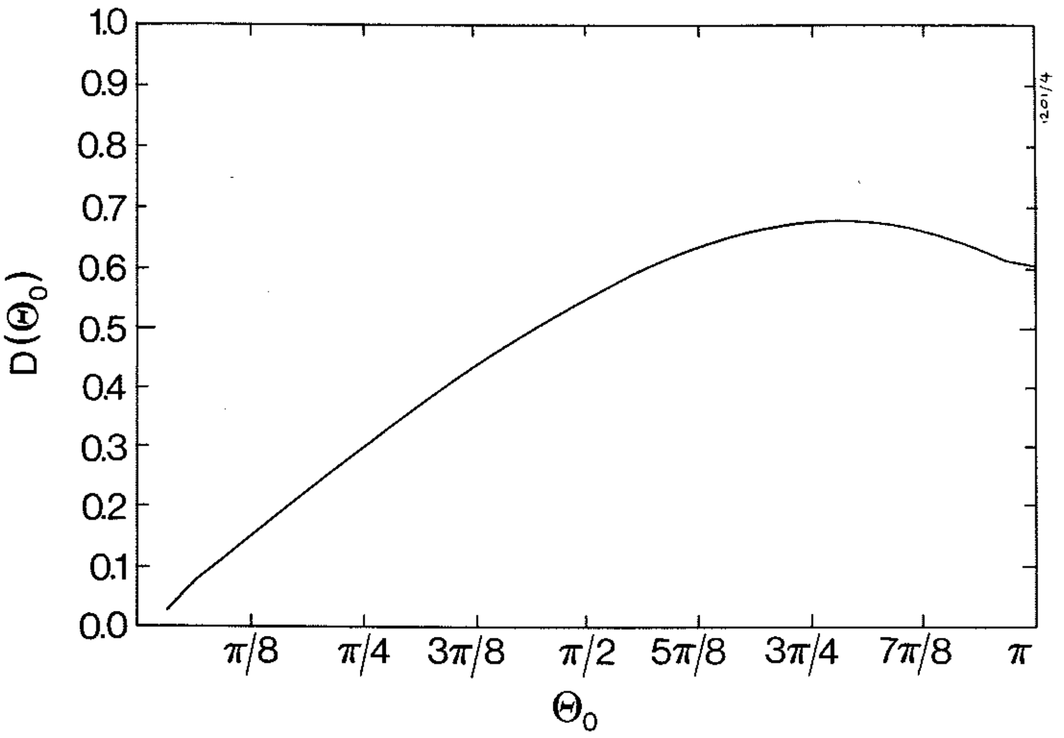

Fig. 4: Function $D(\Theta_0)$ defined by Eq. (40) as a function of Θ_0.

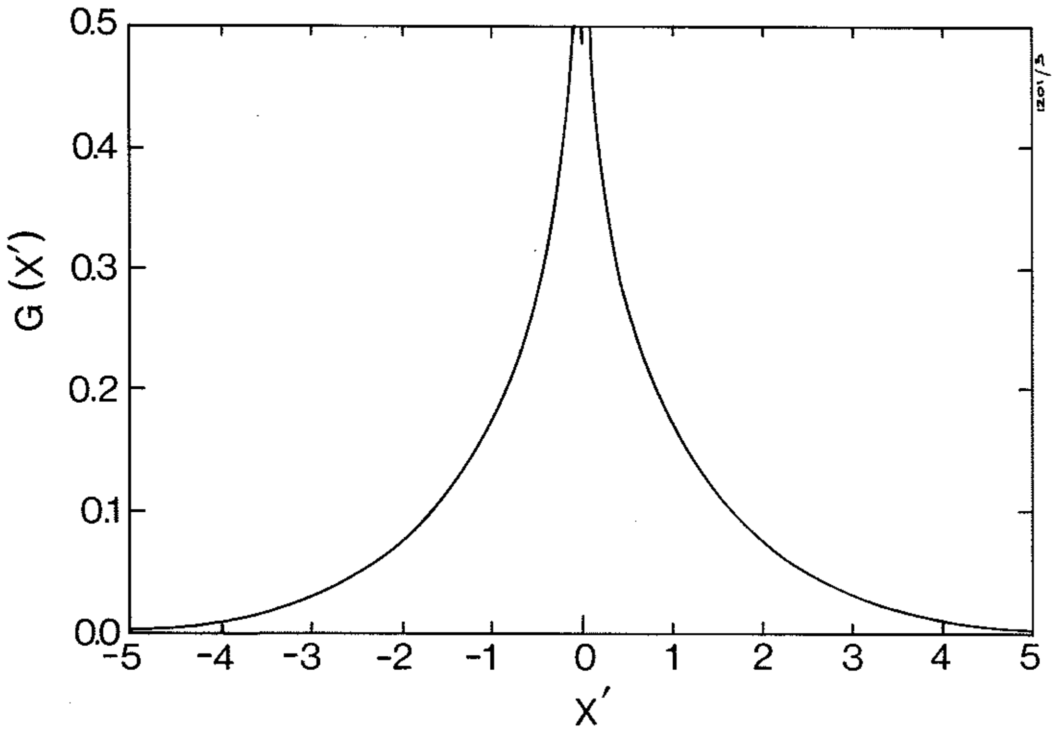

Fig. 5: Variation of $G(x-x')$ given by Eq. (A.5) with x' for $x = 0$ and $\rho_i = 1$; this function enters into the definition of the finite ion Larmor radius operator.

APPENDIX 1.

THE JET TEAM

JET Joint Undertaking, Abingdon, Oxon, OX14 3EA, U.K.

J.M.Adams[1], F.Alladio[4], H.Altmann, R.J.Anderson, G.Appruzzese, W.Bailey, B.Balet, D.V.Bartlett, L.R.Baylor[24], K.Behringer, A.C.Bell, P.Bertoldi, E.Bertolini, V.Bhatnagar, R.J.Bickerton, A.Boileau[3], T.Bonicelli, S.J.Booth, G.Bosia, M.Botman, D.Boyd[31], H.Brelen, H.Brinkschulte, M.Brusati, T.Budd, M.Bures, T.Businaro[4], H.Buttgereit, D.Cacaut, C.Caldwell-Nichols, D.J.Campbell, P.Card, J.Carwardine, G.Celentano, P.Chabert[27], C.D.Challis, A.Cheetham, J.Christiansen, C.Christodoulopoulos, P.Chuilon, R.Claesen, S.Clement[30], J.P.Coad, P.Colestock[6], S.Conroy[13], M.Cooke, S.Cooper, J.G.Cordey, W.Core, S.Corti, A.E.Costley, G.Cottrell, M.Cox[7], P.Cripwell[13], F.Crisanti[4], D.Cross, H.de Blank[16], J.de Haas[16], L.de Kock, E.Deksnis, G.B.Denne, G.Deschamps, G.Devillars, K.J.Dietz, J.Dobbing, S.E.Dorling, P.G.Doyle, D.F.Düchs, H.Duquenoy, A.Edwards, J.Ehrenberg[14], T.Elevant[12], W.Engelhardt, S.K.Erents[7], L.G.Eriksonn[5], M.Evrard[2], H.Falter, D.Flory, M.Forrest[7], C.Froger, K.Fullard, M.Gadeberg[11], A.Galetsas, R.Galvao[8], A.Gibson, R.D.Gill, A.Gondhalekar, C.Gordon, G.Gorini, C.Gormezano, N.A.Gottardi, C.Gowers, B.J.Green, F.S.Griph, M.Gryzinski[26], R.Haange, G.Hammett[6], W.Han[9], C.J.Hancock, P.J.Harbour, N.C.Hawkes[7], P.Haynes[7], T.Hellsten, J.L.Hemmerich, R.Hemsworth, R.F.Herzog, K.Hirsch[14], J.Hoekzema, W.A.Houlberg[24], J.How, M.Huart, A.Hubbard, T.P.Hughes[32], M.Hugon, M.Huguet, J.Jacquinot, O.N.Jarvis, T.C.Jernigan[24], E.Joffrin, E.M.Jones, L.P.D.F.Jones, T.T.C.Jones, J.Källne, A.Kaye, B.E.Keen, M.Keilhacker, G.J.Kelly, A.Khare[15], S.Knowlton, A.Konstantellos, M.Kovanen[21], P.Kupschus, P.Lallia, J.R.Last, L.Lauro-Taroni, M.Laux[33], K.Lawson[7], E.Lazzaro, M.Lennholm, X.Litaudon, P.Lomas, M.Lorentz-Gottardi[2], C.Lowry, G.Magyar, D.Maisonnier, M.Malacarne, V.Marchese, P.Massmann, L.McCarthy[28], G.McCracken[7], P.Mendonca, P.Meriguet, P.Micozzi[4], S.F.Mills, P.Millward, S.L.Milora[24], A.Moissonnier, P.L.Mondino, D.Moreau[17], P.Morgan, H.Morsi[14], G.Murphy, M.F.Nave, M.Newman, L.Nickesson, P.Nielsen, P.Noll, W.Obert, D.O'Brien, J.O'Rourke, M.G.Pacco-Düchs, M.Pain, S.Papastergiou, D.Pasini[20], M.Paume[27], N.Peacock[7], D.Pearson[13], F.Pegoraro, M.Pick, S.Pitcher[7], J.Plancoulaine, J-P.Poffé, F.Porcelli, R.Prentice, T.Raimondi, J.Ramette[17], J.M.Rax[27], C.Raymond, P-H.Rebut, J.Removille, F.Rimini, D.Robinson[7], A.Rolfe, R.T.Ross, L.Rossi, G.Rupprecht[14], R.Rushton, P.Rutter, H.C.Sack, G.Sadler, N.Salmon[13], H.Salzmann[14], A.Santagiustina, D.Schissel[25], P.H.Schild, M.Schmid, G.Schmidt[6], R.L.Shaw, A.Sibley, R.Simonini, J.Sips[16], P.Smeulders, J.Snipes, S.Sommers, L.Sonnerup, K.Sonnenberg, M.Stamp, P.Stangeby[19], D.Start, C.A.Steed, D.Stork, P.E.Stott, T.E.Stringer, D.Stubberfield, T.Sugie[18], D.Summers, H.Summers[20], J.Taboda-Duarte[22], J.Tagle[30], H.Tamnen, A.Tanga, A.Taroni, C.Tebaldi[23], A.Tesini, P.R.Thomas, E.Thompson, K.Thomsen[11], P.Trevalion, M.Tschudin, B.Tubbing, K.Uchino[29], E.Usselmann, H.van der Beken, M.von Hellermann, T.Wade, C.Walker, B.A.Wallander, M.Walravens, K.Walter, D.Ward, M.L.Watkins, J.Wesson, D.H.Wheeler, J.Wilks, U.Willen[12], D.Wilson, T.Winkel, C.Woodward, M.Wykes, I.D.Young, L.Zannelli, M.Zarnstorff[6], D.Zasche[14], J.W.Zwart.

PERMANENT ADDRESS

1. UKAEA, Harwell, Oxon. UK.
2. EUR-EB Association, LPP-ERM/KMS, B-1040 Brussels, Belgium.
3. Institute National des Récherches Scientifique, Quebec, Canada.
4. ENEA-CENTRO Di Frascati, I-00044 Frascati, Roma, Italy.
5. Chalmers University of Technology, Göteborg, Sweden.
6. Princeton Plasma Physics Laboratory, New Jersey, USA.
7. UKAEA Culham Laboratory, Abingdon, Oxon. UK.
8. Plasma Physics Laboratory, Space Research Institute, Sao José dos Campos, Brazil.
9. Institute of Mathematics, University of Oxford, UK.
10. CRPP/EPFL, 21 Avenue des Bains, CH-1007 Lausanne, Switzerland.
11. Risø National Laboratory, DK-4000 Roskilde, Denmark.
12. Swedish Energy Research Commission, S-10072 Stockholm, Sweden.
13. Imperial College of Science and Technology, University of London, UK.
14. Max Planck Institut für Plasmaphysik, D-8046 Garching bei München, FRG.
15. Institute for Plasma Research, Gandhinagar Bhat Gujat, India.
16. FOM Instituut voor Plasmafysica, 3430 Be Nieuwegein, The Netherlands.
17. Commissiariat à L'Energie Atomique, F-92260 Fontenay-aux-Roses, France.
18. JAERI, Tokai Research Establishment, Tokai-Mura, Naka-Gun, Japan.
19. Institute for Aerospace Studies, University of Toronto, Downsview, Ontario, Canada.
20. University of Strathclyde, Glasgow, G4 ONG, U.K.
21. Nuclear Engineering Laboratory, Lapeenranta University, Finland.
22. JNICT, Lisboa, Portugal.
23. Department of Mathematics, Univeristy of Bologna, Italy.
24. Oak Ridge National Laboratory, Oak Ridge, Tenn., USA.
25. G.A. Technologies, San Diego, California, USA.
26. Institute for Nuclear Studies, Swierk, Poland.
27. Commissiariat à l'Energie Atomique, Cadarache, France.
28. School of Physical Sciences, Flinders University of South Australia, South Australia SO42.
29. Kyushi University, Kasagu Fukuoka, Japan.
30. Centro de Investigaciones Energeticas Medioambientales y Techalogicas, Spain.
31. University of Maryland, College Park, Maryland, USA.
32. University of Essex, Colchester, UK.
33. Akademie de Wissenschaften, Berlin, DDR.

CR 88.49.1A